Journal of Membrane Science 563 (2018) 351–359

Contents lists available at ScienceDirect

Journal of Membrane Science

journal homepage: www.elsevier.com/locate/memsci

Hydrogen permeation and surface properties of PdAu and PdAgAu membranes in the presence of CO, CO_2 and H_2S

Agustina Dalla Fontana, Noelí Sirini, Laura M. Cornaglia, Ana M. Tarditi*

Instituto de Investigaciones en Catálisis y Petroquímica, INCAPE, Universidad Nacional del Litoral, CONICET, Facultad de Ingeniería Química, Santiago del Estero 2829, 3000 Santa Fe, Argentina

ARTICLE INFO

Keywords:
Palladium membrane
Ternary alloy
CO
CO_2
H_2S

ABSTRACT

Using the electroless deposition technique with different deposition sequences, it was possible to obtain a single phase PdAgAu ternary alloy after treatment at 773 K during 7 days. Despite the order of deposition, the samples exhibited similar hydrogen permeation flux at the same temperature and pressure. In the presence of CO, the PdAgAu ternary alloy membranes showed a lower inhibition on the hydrogen permeance compared with the binary PdAu alloy at 623 and 673 K. On the contrary, under CO_2 containing streams, the ternary alloy showed a higher inhibition with a complete hydrogen recovery after removing CO_2 from the stream. When H_2S was introduced in the 13% CO_2/13% Ar/74% H_2 stream, a higher permeance decrease was observed on both the PdAu and PdAgAu alloy membranes. After removal of H_2S, a hydrogen recovery of 60% and 76% was measured for the PdAu and PdAgAu membranes, respectively. Pd surface segregation was observed on the $Pd_{82}Ag_{15}Au_3$–873 K-5 d and the $Pd_{78}Au_6Ag_{16}$–773 K-7 d samples upon exposure to CO containing streams. Instead, silver surface segregation was observed by XPS after exposing the PdAgAu ternary alloy to CO_2 containing streams.

1. Introduction

The release of greenhouse gases (GHG) into the atmosphere due to the continuous burning of fossil fuels is a serious threat to the environment leading to the consequent climate change. For a long-term treatment of climate change along with the reduction of the dependence on fossil fuels, future energy sources must meet the requirements of being carbon-free and renewable [1]. In this perspective, hydrogen is emerging as a viable alternative to be used as energy carrier by means of fuel cells. Hydrogen is mainly produced from reforming reactions, in which a purification step is required to increase the hydrogen concentration. The integration of production and purification in a single unit by the implementation of membrane reactors (MRs) turns out as a promising technology for high purity hydrogen production.

The special ability of palladium to dissociate hydrogen to its atomic form makes this metal ideal for hydrogen separation applications [2]. Therefore, palladium-based membranes have received increased attention during the last decade. In his pioneering work, Hunter disclosed that alloying Pd with 27 mass % Ag not only prevented hydrogen embrittlement but also improved hydrogen permeability by 70% compared to pure palladium at 723 K [3,4]. However, Pd and most of its alloys are very sensitive to sulphur compounds even at low ppm levels [5,6]. Even a few ppm of sulphur in the gas reduce the flux drastically due to strong surface adsorption leading to reduced permeability or to the complete deterioration of the membrane caused by the formation of bulk Pd_4S [7]. Hence, in recent years multi-component Pd alloys, which combine good sulphur tolerance with better H_2 permeability and reduced membrane costs, have been explored [8–13]. It has been shown that the addition of a third element to the PdAg alloy improves the tolerance to poisoning with H_2S, maintaining high hydrogen permeability [10]. The PdAgAu alloys exhibited the highest permeability and the lowest post-exposure surface S content after being submitted to a H_2S stream, within a set of PdAgX alloys with X (Au, Mo, Cu and Y), as analyzed by Bredesen et al. [10].

Along with H_2S, CO is another important contaminant normally present when generating H_2 from fossil fuels. Among CO and CO_2, CO is clearly the most inhibiting species [14–18], this effect being attributed to differences in adsorption energy. Additionally, it has been found that a single adsorbed CO molecule can block more than one hydrogen dissociation site [14,19]. In addition, it has also been found that CO increases the hydrogen desorption energy and induces an activation barrier for hydrogen dissociation [14,20]. Several publications have reported the inhibitory effect upon pure Pd and binary Pd-alloys, caused by exposure to a CO rich stream. A strong inhibition has been reported in the presence of CO at low temperatures (548–623 K) due to a competitive adsorption. Wieland et al. [21] studied the influence of

* Corresponding author.
E-mail address: atarditi@fiq.unl.edu.ar (A.M. Tarditi).

https://doi.org/10.1016/j.memsci.2018.06.001
Received 27 November 2017; Received in revised form 30 May 2018; Accepted 1 June 2018
Available online 04 June 2018

CO at different compositions and 573 K for the methanol steam reforming process. Compared to pure hydrogen permeation, the flux decreased by over 70% when the membrane was exposed to CO or methanol. The effects observed suggest that the adsorption of these components on the membrane competes with the adsorption of hydrogen, which is a precondition for hydrogen permeation through palladium membranes. Li et al. [22] reported a similar effect for a Pd/stainless steel membrane. A strong reduction in the hydrogen permeation was observed for mixtures containing CO or steam at 653 K, which was associated with the competitive adsorption of CO or steam on the Pd surface. On the other hand, at higher temperatures CO adsorption and carbon deposition could occur. A strong hydrogen inhibition has been reported upon exposing a PdAg membrane to CO_2 and steam at a temperature range between 623 and 723 K [23], which has been attributed to carbon deposition on the Pd or PdAg surface. Using temperature-programmed oxidation experiments and SEM, Goldbach et al. [24] observed carbon deposits on a Pd membrane upon exposure to CO_2 containing streams.

The aim of this work was to study the inhibition effect caused by the presence of gases CO, CO_2, H_2S and the mixture of these gases on hydrogen permeability over binary and ternary palladium alloys. By means of sequential electroless plating, Pd-based binary and ternary membranes were prepared. The as synthesized membranes were evaluated in a temperature range between 623 and 673 K and a pressure difference of 50 kPa. Characterizations of the Pd-based binary and ternary membranes were performed using DRX, SEM, XPS and LEIS.

2. Experimental

2.1. PdAu and PdAgAu samples preparation

Porous stainless-steel discs were used as supports for the deposition of PdAu and PdAgAu alloy membranes. The supports were provided by Mott Metallurgical Corporation (1.27 cm in diameter, 4 mm thickness and 0.1 μm grade). Before the metallic depositions, the supports were conditioned as reported in our previous published work [25]. Pd-based membranes were prepared by means of electroless plating, using the compositions and temperature previously optimized by our group [13,25]. The metals were deposited on top of the substrates by the sequential deposition method according to the following sequences:

i) Pd-Au, for the binary alloys and
ii) Pd-Au-Ag or Pd-Ag-Au, for the ternary alloys.

In the latter case, two deposition sequences were studied in order to analyze the effect of deposition on the bulk and surface properties of the membranes.

The atomic composition of the samples was modified using different deposition times. After deposition, the samples were heated up to 773 or 873 K in an inert atmosphere (with a heating rate of 1 K min^{-1}) and switched to hydrogen with a difference pressure across the membrane equal to 10 kPa to promote the alloy formation. Throughout the annealing procedure the permeate side was kept at atmospheric pressure. Table 1 shows the main properties of the synthesized samples. The binary samples were labeled as PdAu-M_x (where x refers to the sample number) and the ternary alloys as $Pd_aAg_bAu_c$-X-Y or $Pd_aAu_bAg_c$-X-Y (where a, b, c are the atomic composition, X and Y the temperature and time of thermal treatment, respectively). Note that the position of Ag and Au on the nomenclature changed according to the sequence of deposition.

2.2. Single gas permeation and CO, CO_2 and H_2S inhibition tests

Permeation measurements were carried out using a device designed in our group [26]. The effective permeation area of the membranes was 0.5 cm^2 in all cases. After annealing and hydrogen single gas permeation, the membranes were exposed to CO, CO_2 and H_2S containing streams at 623 and 673 K. During permeation measurements, the permeate side was kept at atmospheric pressure. Table 2 shows the composition of the mixtures studied. The treatment was performed during 6 or 24 h, followed by a hydrogen recovery at the treatment temperature. The pressure difference across the membrane was kept between 45 and 60 kPa. The membrane integrity was checked using pure nitrogen after each set of experiments. To check the dilution effect on the hydrogen permeation through the membranes, a N_2(27%)/H_2 mixture was used.

2.3. Sample characterization

The alloy formation was analyzed by X-ray diffraction (XRD) using a XD-D1 Shimadzu diffractometer, with a Cu Kα (λ = 1.542 Å) radiation operating at 30 kV and 40 mA. The 95% of the information achieved on a XRD pattern of a Pd-based alloy are originated from a depth of 2.2 μm, being the 100% of the X-ray absorbed at a thickness between 4 and 5 μm, as reported by Ma et al. [27].

The surface morphology and thickness were analyzed by Scanning Electron Microscopy (SEM) with a JEOL (JSM-35C) microscope. The cross sectional elemental composition of the samples was performed using a FEI, Quanta 200F microscope, equipped with a field emission gun and a Si(Li) EDS detector of 10 mm^2. The data were processed with a Genesis v6.04 program.

The bulk atomic composition of the samples was determined by X-ray fluorescence spectroscopy (XRF) and SEM-EDS (sampling depth ~ 2– 2.7 μm using an voltage of 30 keV). The XRF data were collected using an EDX-729 Shimadzu Energy Dispersive X-ray spectrometer with a Rh X-ray tube operated at 50 kV, under these conditions the analysis depth are ~ 100 μm. The quantification was performed by a calibration curve using reference samples of known composition prepared by electroless deposition.

The surface properties of the membranes were studied by X-Ray Photoelectron Spectroscopy (XPS) and Low Energy Ions Scattering Spectroscopy (LEIS) using a multi-technique system (SPECS) equipped with a hemispherical PHOIBOS 150 analyzer operating in the fixed analyzer transmission (FAT) mode. The spectra were obtained using a monochromatic Al Kα radiation (hν = 1486.6 eV) operated at 300 W and 14 kV. The spectra of Pd 3d, Pd 3p, O 1s, C 1s, Au 4f, Ag 3d and Fe 2p were recorded for each sample. The data treatment was performed with the Casa XPS program (Casa Software Ltd., UK). The peak areas were determined by integration employing a Shirley-type background. Peaks were considered to be a mixture of Gaussian and Lorentzian functions. Sensitivity factors provided by the instrument manufacturer were used for the quantification of composition. For the LEIS experiments, a differentially pumped ion source IQE 12/38 SPECS, in the multi-technique system was used. The spectra were taken using 1 keV helium ions at a scattering angle of 50°, with a current density of about 400 nA cm^{-2} (1.5×10^{14} ion cm^{-2} to take a complete experiment), given a sputtering rate of 0.01 nm min^{-1} as estimated using the equation reported by Hoffman [28]. Reference samples to calibrate the LEIS signals and to obtain sensitivity factors were pure Pd, Au and Ag foils [29].

3. Results and discussion

3.1. Alloy formation and surface composition

In a previous publication, we reported that after annealing a sample of ~ 10 μm thickness at 773 K during 5 days, the formation of a partial fcc PdAgAu alloy was observed by XRD [13]. All the reflection peaks exhibited a shoulder at higher values of 2θ. A subsequent annealing up to 873 K for 2 days yielded a XRD pattern with symmetrical peaks (Fig. 1). In order to optimize the alloy formation at a lower temperature (773 K), in the present work the ternary alloy samples were annealed at

Table 1
Chemical atomic composition of the synthesized samples.

Sample	(at%) XRF			(at%) EDS			(at%) XPS			Thickness (μm)	
	Pd	Ag	Au	Pd	Ag	Au	Pd	Ag	Au	XRF	SEM
PdAu-M1	95.0	–	5.0	93.5	–	6.5	97.2	–	2.8	14	13
PdAu-M2	97.7	–	2.3	96.0	–	4.0	96.0	–	4.0	15	–
PdAu-M3	96.2	–	3.8	–	–	–	–	–	–	15	–
$Pd_{69}Ag_{24}Au_7$–873 K-5 d	69.4	23.4	7.2	68.6	24.1	7.3	51.6	41.2	7.2	10	11
$Pd_{82}Ag_{15}Au_3$–873 K-5 d	–	–	–	81.8	14.9	3.3	59.7	37.5	2.8	14	14
$Pd_{91}Au_3Ag_6$–773 K-7 d	–	–	–	90.9	6.3	2.8	80.1	17.2	2.7	–	–
$Pd_{78}Au_6Ag_{16}$–773 K-7 d	78.2	16.1	5.7	–	–	–	77.7	19.9	2.4	–	–
$Pd_{78}Au_8Ag_{14}$–773 K-7 d	77.3	13.5	9.2	77.9	13.8	8.3	74.1	16.8	9.1	13	–
$Pd_{76}Au_{10}Ag_{14}$–773 K-7 d	76.0	13.9	10.1	–	–	–	–	–	–	14	–
$Pd_{76}Ag_{15}Au_9$–773 K-7 d	–	–	–	76.3	15.1	8.6	76.0	21.0	3.0	–	–
$Pd_{81}Ag_{16}Au_3$–773 K-7 d	–	–	–	81.0	15.7	3.3	–	–	–	–	15

Table 2
Composition of the mixtures studied.

Mixture	Feed composition
(i)	1.25% CO/23.75% He/75% H_2
(ii)	1.25% CO/23.75% He/75% H_2/75 ppm H_2S
(iii)	13% CO_2/13% Ar/74% H_2
(iv)	13% CO_2/13% Ar/74% H_2/74 ppm H_2S
(v)	27% N_2/73% H_2

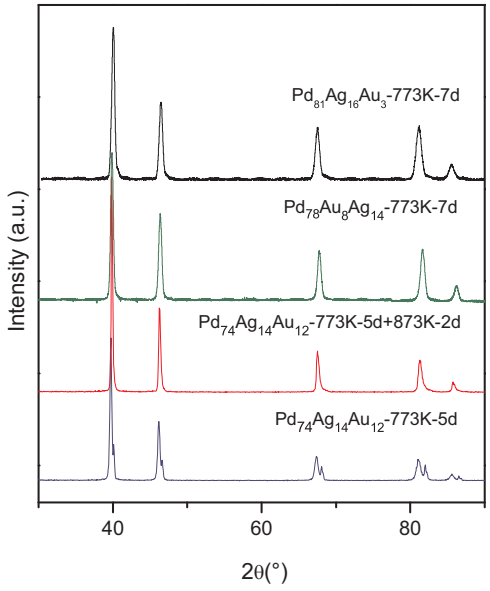

Fig. 1. Effect of the temperature, annealing time and metal sequence deposition on the ternary alloy formation.

773 K during 7 days under hydrogen flux and a pressure difference across the membrane equal to 10 kPa, keeping the permeate side at atmospheric pressure. The XRD diffraction patterns of the $Pd_{78}Au_8Ag_{14}$–773 K-7 d and the $Pd_{81}Ag_{16}Au_3$–773 K-7 d samples are presented in Fig. 1 in comparison with those obtained for samples $Pd_{74}Ag_{14}Au_{12}$–773 K-5 d and $Pd_{74}Ag_{14}Au_{12}$–773 K-5 d-873 K-2 d. Note that the annealing up to 773 K during 7 days gave an X-ray diffraction pattern with symmetric peaks for both the $Pd_{78}Au_8Ag_{14}$–773 K-7 d and $Pd_{81}Ag_{16}Au_3$–773 K-7 d samples, without shoulders in the XRD analysis depth. This gives us an indication that the order of metallic deposition does not directly influence the alloy formation at 773 K during 7 days in a pure hydrogen stream and 10 kPa. Lewis et al. [9] reported a non-homogeneous alloy formation after annealing a sample with the Pd-Au-Ag deposition sequence at 773 K during 5 days under a 3.5%H_2/Ar stream. Using gravimetric methods, the authors estimated a thickness of 9.3 μm in the ternary alloy. On the contrary, by annealing an electroless deposited PdAgAu membrane up to 1023 K during 2 h, Pacheco Tanaka et al. [30] reported a complete alloy formation for samples with a thickness of ca. 1.0 μm. For the samples prepared in this work, we achieved complete alloy formation at a lower temperature during a moderate period of time, applying a pressure difference of 10 kPa across the membrane. A complete alloy formation for a PdAu film at 723 K in only 2 days by increasing the hydrogen pressure above 3 MPa at the feed side of the membrane has been recently reported [31]. Using SEM, XRF and gravimetric methods, the authors reported a thickness of ~ 4.9 μm was estimated for this PdAu film.

To determine the homogeneity in composition through the thickness of the alloy films, EDS line scan has been performed on the cross-section of the $Pd_{76}Au_{10}Ag_{14}$–773 K-7 d and $Pd_{81}Ag_{16}Au_3$–773 K-7 d samples annealed at 773 K. As shown in Fig. 2, despite the metal deposition sequence used, the samples exhibited a homogeneous elemental distribution on thickness, which could confirm the alloy formation in agreement with the XRD observations (Fig. 1).

The atomic bulk composition of the samples was determined by EDS and XRF. In order to determine the homogeneity of the alloy, five determinations were performed at difference points through the top view of the membranes, showing a homogeneous composition in all the samples. The bulk composition and thickness of the membranes are summarized in Table 1, the reported composition being an average value of the five data obtained for each sample. Note that all the samples showed an alloy thickness between 10 and 15 μm, which was confirmed by SEM and XRF (Table 1).

The SEM images of the as synthesized $Pd_{91}Au_3Ag_6$–773 K-7 d and $Pd_{78}Au_8Ag_{14}$–773 K-7 d samples are shown in Fig. 3. Both samples exhibit a globular microstructure similar to the morphology of samples prepared by the electroless method. On the top view, it is possible to observe the formation of larger structures, which could be related to the dendritic growth of silver by electroless deposition [32]. Note that the size of these structures is higher for the sample with a higher silver content ($Pd_{78}Ag_{14}Au_8$–773 K-7 d).

The XPS surface atomic composition of the ternary alloy as synthesized samples increases significantly with respect to the bulk composition (XRF and EDS, Table 1). For the $Pd_{69}Ag_{24}Au_7$–873 K-5 d alloy, the silver surface composition was 41.2% while the bulk composition was 24.1%. On the other hand, for the $Pd_{82}Ag_{15}Au_3$–873 K-5 d sample with a Ag atomic composition of 15%, the surface composition was as high as 37.5%, showing that the higher the silver bulk composition, the higher surface silver segregation occurs. Despite the deposition sequence used for the membrane synthesis (Pd-Ag-Au or Pd-Au-Ag), the surface composition of samples with a similar bulk concentration is quite equal (Table 1).

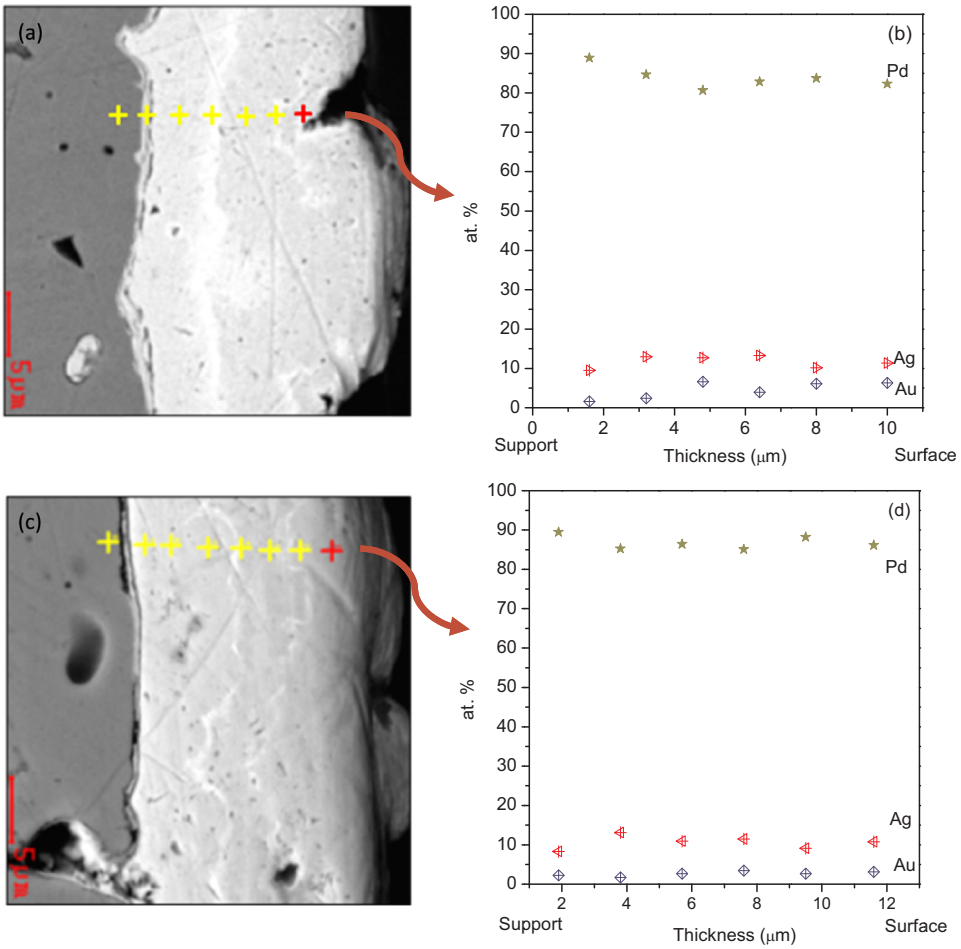

Fig. 2. Cross-sectional EDS scans for the $Pd_{76}Au_{10}Ag_{14}$–773 K-7 d (a, b) and $Pd_{81}Ag_{16}Au_3$–773 K-7 d (c, d) samples.

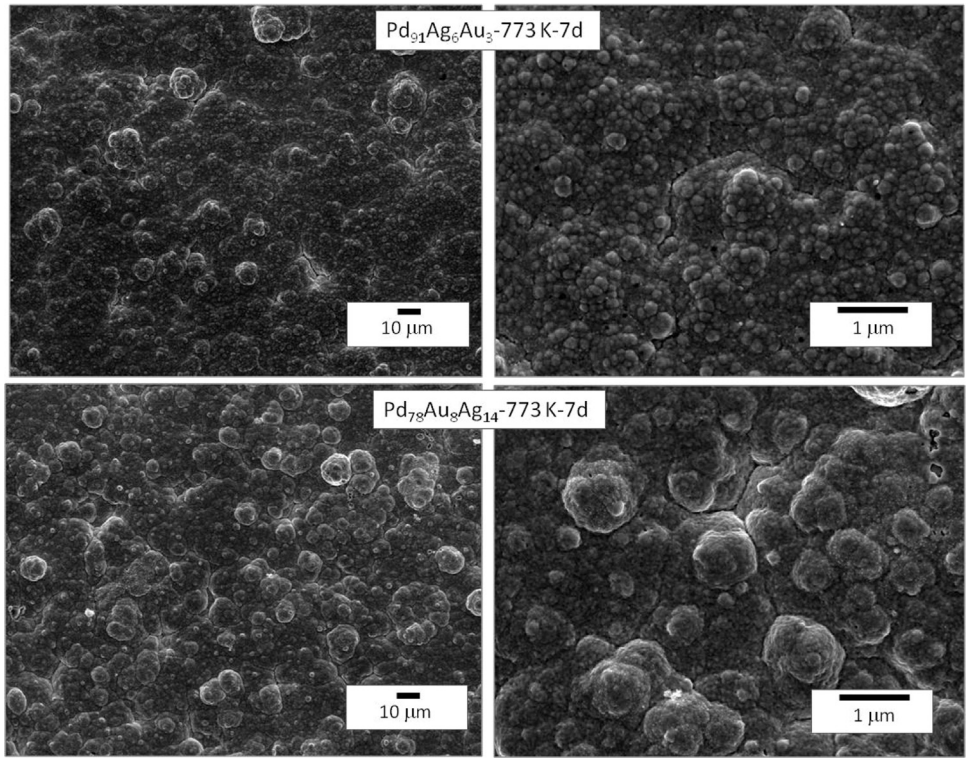

Fig. 3. Top surface morphology of the $Pd_{91}Au_3Ag_6$–773 K-7 d and $Pd_{78}Au_8Ag_{14}$–773 K-7 d samples after alloy formation.

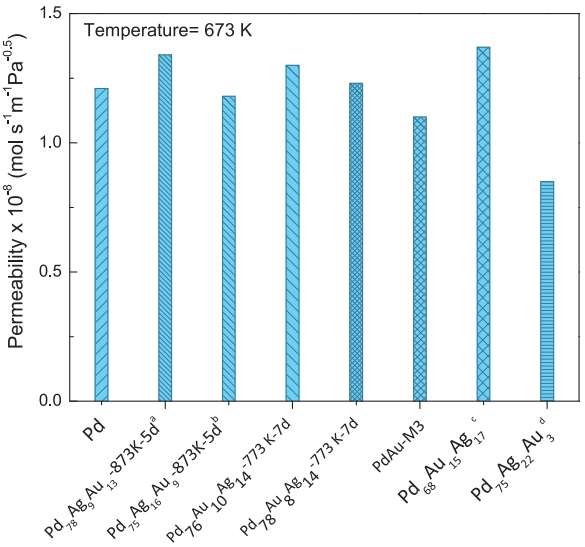

Fig. 4. Comparison of the hydrogen permeability for the samples prepared in this work with those previously reported. The data of the $Pd_{78}Ag_9Au_{13}$–873 K-5 d[a] and $Pd_{75}Ag_{16}Au_9$–873 K-5 d[b] samples were taken from Ref. [12], and those of the $Pd_{68}Au_{15}Ag_{17}$[c] and $Pd_{75}Ag_{22}Au_3$[d] from Refs. [9,10], respectively. Data were reported at 623 K.

3.2. Permeation properties in the presence of CO, CO_2 and H_2S

The flux inhibition under the presence of contaminants was analyzed by feeding different mixtures to the permeator, as shown in Table 2. The experiments were performed at two temperatures, 623 K and 673 K, and a pressure difference across the membrane equal to 50 kPa. In all cases, the permeate was kept at atmospheric pressure. Before studying the effect of contaminants, H_2 and N_2 single gas permeation experiments were carried out in order to study the performance of the membranes. For all the membranes studied, the hydrogen flux yielded a linear dependence with ($P_{ret}^{0.5} - P_{perm}^{0.5}$), which is in agreement with the solution-diffusion mechanism proposed for the Pd-based membranes. For the sake of comparison, Fig. 4 shows the hydrogen permeability at 673 K of our PdAu and PdAgAu membranes and those previously reported. It is important to note that despite the deposition sequence used during the deposition of the ternary alloy membranes, the hydrogen permeabilities of the membranes are higher than the permeability of the PdAu alloy, in agreement with the data previously reported [9,12]. These PdAgAu ternary alloys showed excellent properties in the presence of H_2S, with no evidence of sulphur species in the bulk as determined by XRD [9,10].

It is known that CO, a gas presented in the reformer reactors, has a competitive effect on the adsorption sites at the Pd alloy surface, with a consequent inhibition of hydrogen permeation through the membrane [33]. In the present work, we analyzed the effect of CO with and without the addition of H_2S, on the permeation properties of PdAu and PdAgAu alloy membranes. Fig. 5a shows the hydrogen permeance evolution as a function of time when the sample PdAu-M3 was exposed to a 1.25% CO/23.75% He/75% H_2 stream during 6 h at 623 K and 673 K. After 6 h, hydrogen was fed to the reactor to study the recovery at the same temperature and pressure (Fig. 5). At 673 K, the membrane exhibited a H_2 permeance of 1.8×10^{-2} mol s^{-1} m^{-2} $kPa^{-0.5}$. Upon exposure to CO, at this temperature and ΔP, the membrane evidenced a reduction of ca. 84% in the hydrogen permeance, reaching a steady state after two hours at a value of 0.3×10^{-2} mol s^{-1} m^{-2} $kPa^{-0.5}$. When the treatment was performed at 623 K under the same conditions, a higher inhibition in the hydrogen permeance was observed (ca. 89%, Fig. 5a). The membrane presented a hydrogen recovery of almost 100% after 1 h of hydrogen exposure at the two temperatures evaluated. The high reduction in the permeance upon CO exposure could be associated with the formation of strongly adsorbed species instead of a competitive adsorption as reported by Mejdell et al. [14] for PdAg membranes. These data are in agreement with those reported in the literature, in which a higher inhibition effect was observed increasing the CO concentration and decreasing the temperature for Pd membranes [18]. These authors also reported a sharp drop between 39% and 84% in the hydrogen permeation through a PdAg membrane under exposure to 0.25 mol% of CO at 548–623 K.

The evolution of hydrogen permeance under exposure to 13.5 mL min^{-1} of CO (5%)/He and a 40 mL min^{-1} H_2 stream for the $Pd_{76}Au_{10}Ag_{14}$–773 K-7 d membrane is shown in Fig. 5b. The treatment was performed during 6 h at 623 K and 673 K. Note that the hydrogen permeance quickly dropped up to about a 36% lower of the original permeance (2.5×10^{-2} mol s^{-1} m^{-2} $kPa^{-0.5}$) when the treatment was performed at 623 K. When hydrogen was fed back to the reactor, an almost complete hydrogen recovery was observed. Contrary to the observed on the PdAu membrane (Fig. 5a), the hydrogen permeation of the $Pd_{76}Au_{10}Ag_{14}$ membrane did not change significantly upon exposure to CO mixture at 673 K (Fig. 5b). The hydrogen permeation before CO exposure was 0.025 mol s^{-1} m^{-2} $kPa^{-0.5}$; immediately CO was fed to the permeator, the permeance increases up to 0.037 mol s^{-1} m^{-2} $kPa^{-0.5}$ and quickly stabilizes at a value of 0.025 mol s^{-1} m^{-2} $kPa^{-0.5}$.

After 48 h of hydrogen exposure, the membrane was fed with a 1.25% CO/23.75% He/75% H_2/75 ppm H_2S mixture at 623 K. Note that the hydrogen permeance dropped by a 54% of the original permeance, showing a higher inhibition with the presence of H_2S on the stream. After six hours of treatment, the feed was switched to pure hydrogen at the same temperature (Fig. 5b). A recovery of about 64% of the original permeance was obtained after two hours.

Fig. 6 shows the data obtained as a function of exposure time at streams containing CO_2 with and without the addition of H_2S, for the PdAu-M3 membrane. First, the membrane was fed with a 13% CO_2/13% Ar/74% H_2 mixture stream at 673 K. Note that under these conditions, the hydrogen permeance did not decline. After CO_2 was removed from the stream, pure hydrogen was fed during 24 h. Then, the temperature was lowered up to 623 K and the CO_2 treatment was performed under the same feed composition and pressure. At this temperature, the membrane presented a similar behavior than that observed at 673 K.

After the CO_2 inhibition analysis, the effect of a $CO_2/H_2S/H_2$ mixture was studied. In a first stage, the PdAu-M3 membrane was fed with a 13% CO_2/13% Ar/74% H_2/74 ppm H_2S mixture stream at 623 K for six hours. Note that after six hours of exposure, the hydrogen permeance dropped up to about a 66% of the original permeance at 623 K. After that, hydrogen was fed to the permeator at the same temperature and the hydrogen recovery was analyzed. As shown in Fig. 6, a 72% of the original permeance was reached after about three hours of H_2 exposure. Increasing the temperature up to 773 K during 12 h allowed us to recover an almost 100% of the original permeance at 623 K (Fig. 6). The membrane was exposed to a second cycle feeding a 13% CO_2/13% Ar/74% H_2/74 ppm H_2S mixture stream at 623 K, for 24 h. It is important to note that the permeance fell by up to about 61% of the original value.

Fig. 7 shows the hydrogen permeance evolution upon exposure to CO_2/H_2 and $CO_2/H_2S/H_2$ mixtures at 623 K for the $Pd_{78}Au_8Ag_{14}$–773 K-7 d sample. When CO_2 was fed to the permeator, a sharp drop in the hydrogen permeance was observed, almost up to about 17% of the original permeance. After three hours of exposure, the permeance increased slightly up to 30% and remained in this value (Fig. 7). Immediately, the CO_2 was removed from the stream, the permeance suddenly increased up to about 8% above the original value at the same temperature. After that, during the first hours of recovery the permeance dropped again up to about 99% of the original value. In a second cycle, the effect of a 13% CO_2/13% Ar/74% H_2/74 ppm H_2S mixture stream at 623 K was evaluated. In this case, the permeance

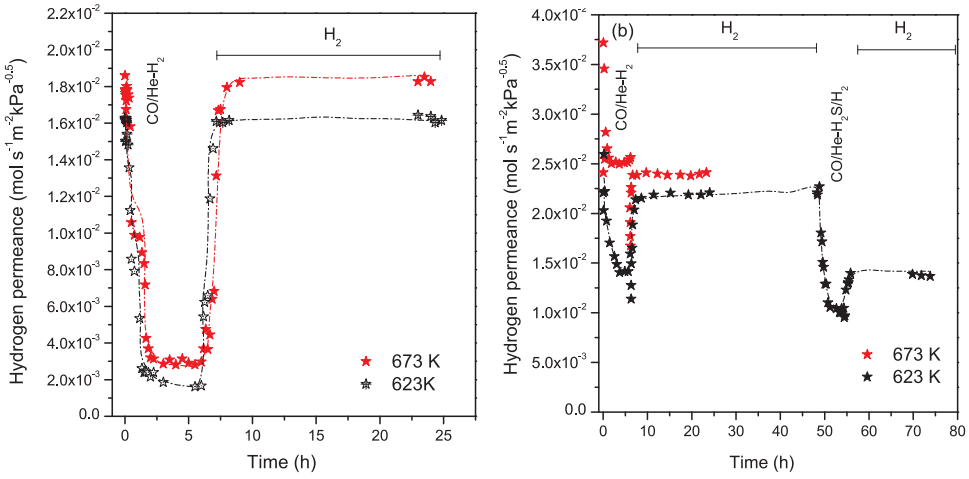

Fig. 5. Evolution of the hydrogen permeance under 1.25% CO/23.75% He/75% H_2 exposure for samples (a) PdAu-M3 and (b) $Pd_{76}Au_{10}Ag_{14}$–773 K-7 d.

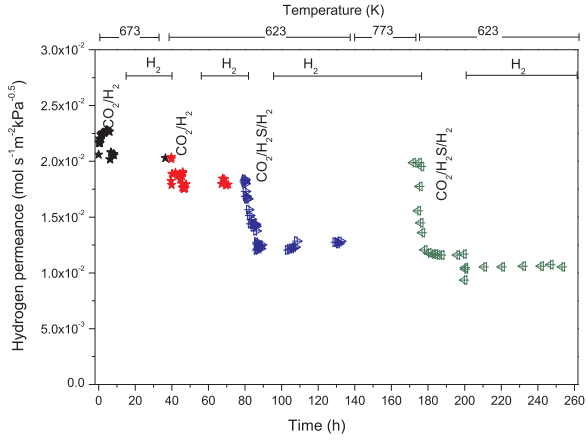

Fig. 6. Evolution of the hydrogen permeance for the PdAu-M3 membrane under 13% CO_2/13% Ar/74% H_2 and 13% CO_2/13% Ar/74% H_2/74 ppm H_2S stream.

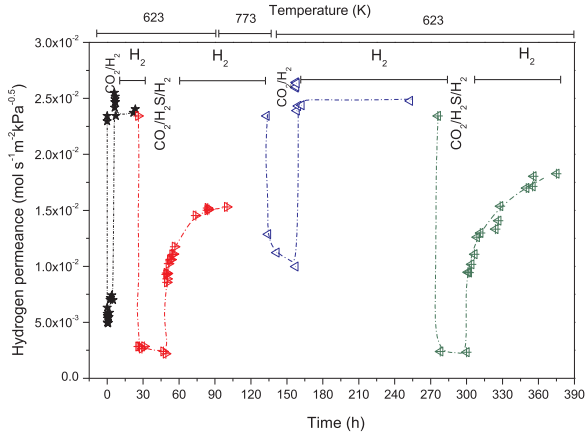

Fig. 7. Evolution of the hydrogen permeance for the $Pd_{78}Au_8Ag_{14}$–773 K-7 d membrane under 13% CO_2/13% Ar/74% H_2 and 13% CO_2/13% Ar/74% H_2/74 ppm H_2S stream.

sharply dropped up to about 8% of the original value and remained under this condition during 24 h of exposure. Then, when the mixture was removed, the permeance increased in two stages: *i)* first quickly up to about 40% of the original value and then in a slower stage with an increase up to 66% after about 24 h of hydrogen recovery and remained constant (Fig. 7). This marked effect on the hydrogen inhibition upon exposure to CO_2 for the PdAgAu ternary alloy, compared with the PdAu binary alloy, could be related to a higher segregation of silver to the surface. A higher concentration of silver on the surface could decrease the dissociation sites on the alloy surface or change the reactivity of the surface for hydrogen dissociation and consequently the hydrogen permeation. After the treatment under 13% CO_2/13% Ar/74% H_2/74 ppm H_2S and hydrogen recovery, the membrane was heated up to 773 K during 12 h (Fig. 7). Note that a complete hydrogen recovery was obtained after that treatment. Then, the sample was submitted to a second cycle of treatment showing a similar behavior to the first one (Fig. 7).

The effect of CO_2 and CO_2 + H_2S on the $Pd_{76}Ag_{15}Au_9$–773 K-7 d membrane was also analyzed (Fig. 8). Note that even though this membrane was obtained with a difference deposition sequence, it exhibited a similar hydrogen permeance (2.5×10^{-2} mol s^{-1} m^{-2} $kPa^{-0.5}$, at 623 K) to the $Pd_{78}Au_8Ag_{14}$–773 K-7 d membrane (2.3×10^{-2} mol s^{-1} m^{-2} $kPa^{-0.5}$). When the $Pd_{76}Ag_{15}Au_9$–773 K-7 d sample was exposed to a 13% CO_2/13% Ar/74% H_2 mixture at 623 K, a sharp drop in the permeance up to 0.9×10^{-2} mol s^{-1} m^{-2} $kPa^{-0.5}$ (about a 36% of the initial value) took place. After that, the membrane had a 100% of hydrogen recovery at the same temperature and pressure. When the sample was exposed at a 13% CO_2/13% Ar/74% H_2/74 ppm H_2S stream, the hydrogen permeance dropped up to about 0.5×10^{-2} mol s^{-1} m^{-2} $kPa^{-0.5}$. A hydrogen recovery of about 76% was obtained after 20 h of hydrogen exposure at the same temperature (Fig. 8). Nitrogen permeation measurements were carried out after different treatments for all membranes. The N_2 flow rate was below the detection limit of the bubble flow meter, which implied an H_2/N_2 ideal selectivity

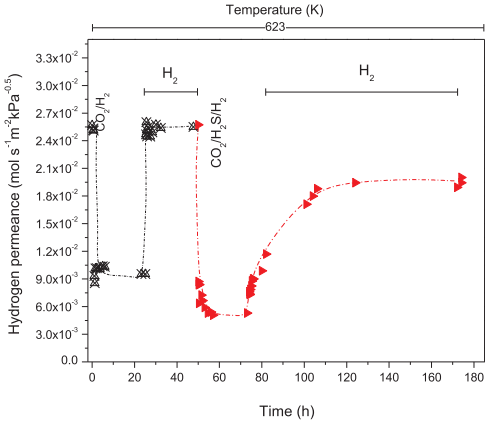

Fig. 8. Evolution of the hydrogen permeance for the $Pd_{76}Ag_{15}Au_9$–773 K-7 d membrane under 13% CO_2/13% Ar/74% H_2 and 13% CO_2/13% Ar/74% H_2/74 ppm H_2S stream at 623 K.

higher than 10,000 as was reported earlier [26]. This result suggests that the membranes were stable under CO, CO_2 and H_2S containing streams, followed by hydrogen recovery, at the applied concentration and exposure times.

It has been reported that the inhibition effect of CO and CO_2 could be assigned to i) the competitive adsorption (at low temperature) or ii) the carbon deposition on the Pd-alloy surface, which is more important at higher temperature [33]. The formation of carbonaceous species has been detected by XRD on Pd-based membranes after exposure to H_2/CO_2 mixtures [34]. Hydrogen inhibition through a PdAg membrane in the presence of CO_2 was shown at temperatures between 548 and 723 K [17]. The authors reported a remarked effect of thickness on the extent of flux decrease on the presence of contaminants like CO and CO_2. Carbon or carbon compounds present at the membrane surface can be partially oxidized by CO_2, which will increase the activity of the Pd for the dissociation of hydrogen and association of H-atoms. For the PdAg membrane, the addition of CO_2 may suppress or increase the preference of Ag for the surface, which will lead to a change in the number of free Pd sites for hydrogen dissociation [17]. On the other hand, the inhibition effect of CO_2 has been assigned to a combination of carbon deposition and the formation of CO and H_2O by the reverse water gas shift (WGS) reaction on the membrane surface [23]. In our case, after exposure to CO and CO_2 streams, not carbon species has been detected by XPS.

Lewis et al. [9] evaluated a $Pd_{67}Au_{20}Ag_{13}$ membrane feeding a simulated water gas shift stream with and without the addition of 20 ppm of H_2S at 673 and 773 K. At both temperatures, the membrane retained a higher permeance compared with a $Pd_{77}Au_{23}$ membrane, under the same conditions. However, similar to our observations, the ternary alloy membrane showed a higher inhibition than the binary alloy [9]. After removing the H_2S from the feed, a 97% of hydrogen recovery was reported by the authors for the ternary alloy. In our case, we obtained a lower hydrogen recovery between 72% and 80% for the ternary alloy, which could be due to the lower temperature of treatment studied or the higher H_2S concentration (74 ppm). On the other hand, PdAgAu membranes with a similar composition showed high resistance to H_2S, even after exposure to 1000 ppm H_2S/H_2 for 30 h, without formation of sulphur species [13]. Upon exposure to 100 ppm H_2S/H_2 at 673 K and 50 kPa, a membrane with a $Pd_{75}Ag_{16}Au_9$ composition, exhibited a flux reduction up to 27% and a hydrogen recovery of about 80% after 30 h [12].

In order to analyze the effect of dilution or the concentration polarization on the hydrogen permeation, a N_2(27%)/H_2 mixture (H_2 feed rate 40 mL min^{-1}, N_2 feed rate 15 mL min^{-1}) was fed to the permeator at 623 K for the $Pd_{76}Ag_{15}$ Au_9–773 K-7 d membrane. Note that, the hydrogen permeation flux presented a linear dependence with ($P_{ret}^{0.5}$-$P_{perm}^{0.5}$) for both pure hydrogen and the N_2:H_2 mixture (Fig. 9), without deviation from the Sieverts law in the pressure range studied. Fig. 9 showed that comparing the data at the same hydrogen partial pressure the permeation flux are the same on both experiments. The addition of nitrogen to the stream decreased the hydrogen partial pressure and consequently the driving force to the permeation. It is important to note that no N_2 permeation was detected for the $Pd_{76}Ag_{15}$ Au_9–773 K-7 d membrane, after the permeation experiments were performed. Abate et al. [35] reported a decrease in the hydrogen permeation under H_2:N_2 mixtures, greater than that expected from a dilution effect. The authors also found a decrease in the separation coefficient from 400 to < 200 at 623 K and 723 K, respectively, showing that the evaluated membrane was not stable at this temperature. Considering these results, it is possible to make a real comparison between the different experiments carried out feeding to our reactor several streams. Note that the hydrogen concentration in the different mixtures reported in Table 2 is about 75%, given the same driving force to permeation. It is known that concentration polarization effect on hydrogen permeation through palladium membrane could be present [36]. The data shown in Fig. 9, suggested that not mass transfer from the external gas phase was present in the permeation experiments performed. The hydrogen recovery factor of the membranes was about 5–6% considering the feed rates and temperatures studied.

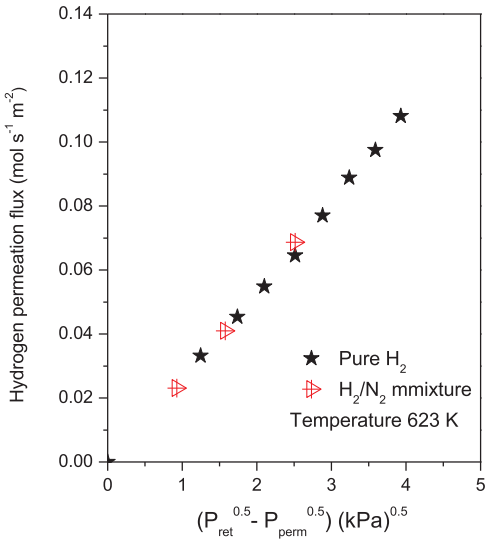

Fig. 9. Hydrogen permeation flux as a function of ($P_{ret}^{0.5}$-$P_{perm}^{0.5}$) for pure hydrogen and a N_2 (27%)/H_2 mixture through the $Pd_{76}Ag_{15}Au_9$–773 K-7 d membrane. Temperature: 623 K.

3.3. Surface properties of the binary and ternary alloy upon exposure to CO and CO_2

To study the effect of CO and CO_2 on the surface properties of the PdAu and PdAgAu alloys, the PdAu-M2 and $Pd_{82}Ag_{15}Au_3$–873 K-5 d samples were exposed to different treatments in the pre-treatment chamber of the spectrometer. To do so, the samples were cut in small pieces and each one exposed to different atmospheres. All the treatments were performed at ambient pressure and at 623 K. Additionally, the atomic surface composition of the $Pd_{78}Au_6Ag_{16}$–773 K-7 d sample was evaluated after three ex-situ treatments: i) annealing ii) CO(5%)/He at 623 K, 4 h and iii) and 1.25% CO/23.75% He/75% H_2 at 623 K, 4 h.

Fig. 10 shows the atomic surface composition of PdAu-M2 (a) and $Pd_{82}Ag_{15}Au_3$–873 K-5 d (b) after being exposed to the different atmospheres. Note that the surface composition of the PdAu binary membrane did not experiment a major change, showing a Au relative composition of about 4% at the surface (Fig. 10a). On the contrary, the ternary alloy showed a higher silver composition (35 at%, Fig. 10b) with respect to the bulk composition (15 at%) after reduction, showing a silver surface enrichment under these conditions. When the sample was exposed to a CO(5%)/He atmosphere at 623 K, the surface composition was quite similar to the bulk composition determined from XRF (Table 1). After exposure to CO_2(20%)/Ar a higher silver enrichment at the surface was observed, giving a Ag surface composition of 42 at% (Fig. 10b). It is important to note that the gold composition remained practically constant about a value of 3 at%. The higher suppression on the hydrogen permeance upon exposure to CO_2 for the $Pd_{78}Au_8Ag_{14}$–773 K-7 d membrane with respect to the PdAu membrane (Figs. 7 and 6, respectively) could be due to the preferential surface silver segregation. The silver enrichment at the surface decreased the number of hydrogen dissociation sites and enhanced the adsorption competition by CO_2. Gielens et al. [23] reported a stronger inhibition of the hydrogen flux upon exposing a PdAg membrane to a CO_2 20 vol %/H_2 stream compared with a Pd membrane. The authors correlated this performance with a silver surface segregation [23]. The authors additionally reported the formation of carbonaceous deposits on the membrane surface.

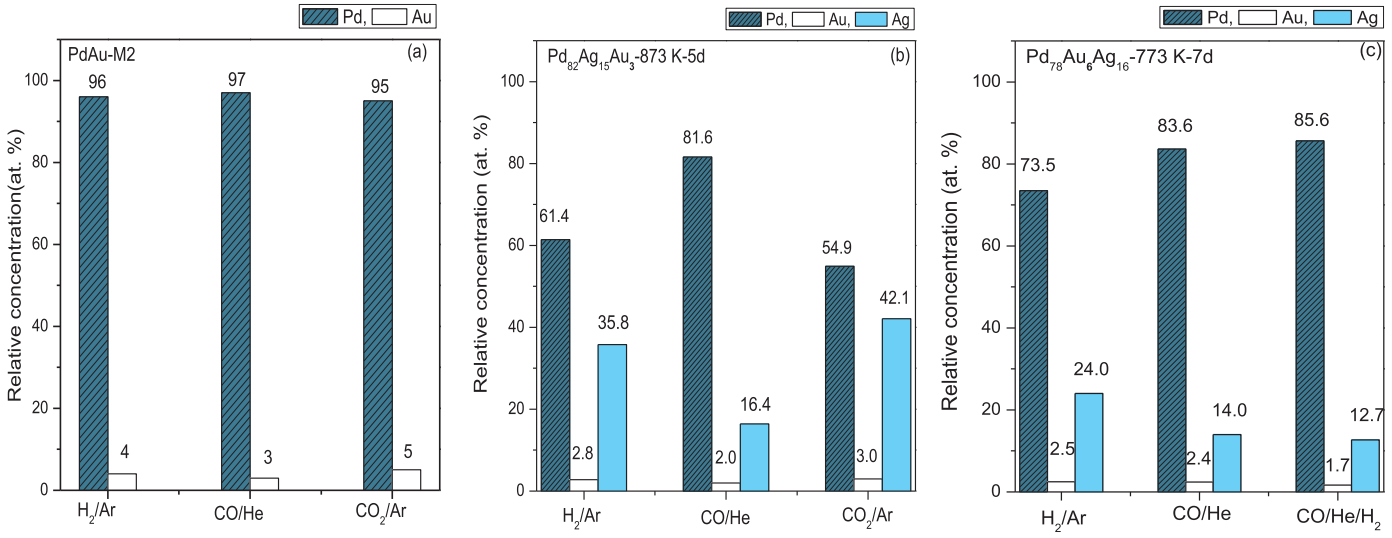

Fig. 10. XPS atomic surface composition of the (a) PdAu-M2 and (b) $Pd_{82}Ag_{15}Au_3$–873 K-5 d after different treatments on the pre-treatment chamber of the spectrometer and (c) for the $Pd_{78}Au_6Ag_{16}$–773 K-7 d after ex-situ treatment on a flow quartz reactor.

By comparing the data obtained for the $Pd_{78}Au_6Ag_{16}$–773 K-7 d membrane with those obtained on the $Pd_{82}Ag_{15}Au_3$–873 K-5 d sample, it is possible to note that the surface composition of both samples after exposure to a CO(5%)/He atmosphere was quite similar, showing a palladium surface enrichment in both cases (Fig. 10b and c). These findings are in agreement with the reverse surface segregation reported for PdAg samples upon exposure to CO [37]. From density functional theory calculations, the authors predicted a silver surface segregation upon vacuum for a PdAg membrane with 23% of silver composition. Upon exposure to hydrogen and carbon monoxide a reverse silver segregation was found, with an increase in the palladium composition on the surface [37]. No significant changes in binding energy and fwhm (full width at half maximum) of the Pd $3d_{3/2}$, Ag $3d_{5/2}$ and Au $4f_{7/2}$ peaks were observed after all the treatments.

Fig. 11 shows the variation in the gold concentration on the near surface region as a function of the He^+ exposure time for the $Pd_{82}Ag_{15}Au_3$–873 K-5 d sample after different treatments. Note that after the treatment in H_2(5%)/Ar, the Au concentration increased with exposure time from 1.4% to 3.9%, showing that Pd and/or Ag segregate to the topmost surface layer, in agreement with the XPS data (Fig. 10b). The same behavior was observed after the treatment in CO_2 containing stream (Fig. 11a). On the other hand, when the sample was exposed to a CO stream, no major variation in the Au concentration was observed in the near surface region as determined by LEIS (Fig. 11a). For the PdAu-M2 sample, the gold composition in the near surface region (determined by LEIS) was almost constant with the exposure time (Fig. 11b) after CO or CO_2 treatment.

After the permeation experiments under a 13% CO_2/13% Ar/74% H_2/74 ppm H_2S stream, the surface composition of the $Pd_{78}Au_8Ag_{14}$–773 K-7 d and PdAu-M3 membranes was analyzed by XPS. The data showed a marked palladium surface enrichment for the $Pd_{78}Au_8Ag_{14}$–773 K-7 d membrane under this condition, with an atomic surface composition of Pd 92.0%, Ag 5.2% and Au 2.8%. The binary alloy did not show a significant change in the surface composition with a palladium atomic concentration of 93.6% after treatment. An increase in the Pd composition for $Pd_{86}Au_{14}$ and $Pd_{68}Au_{15}Ag_{17}$ membranes after treatment in a synthetic WGS mixture with 20 ppm of H_2S was reported by Way et al. [9]. By EDS analysis, the authors reported an atomic composition of Pd 68%, Au 15%, Ag 17% and Pd 79%, Au 11%, Ag 10%, before and after treatment, respectively [9]. However, these results could suggest the formation of a non-homogeneous alloy, in agreement with the asymmetric peaks observed in the XRD patterns of

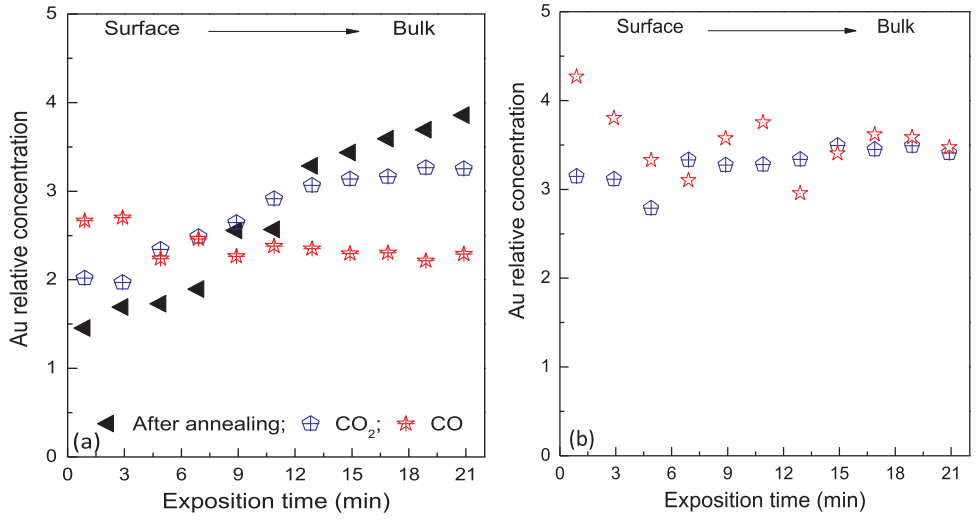

Fig. 11. Au relative composition on the topmost surface layer determined by LEIS for the (a) $Pd_{82}Ag_{15}Au_3$–873 K-5 d and (b) PdAu-M2 samples after different treatments in the pre-treatment chamber of the spectrometer.

the samples [9].

Although the PdAgAu alloy has shown promising results in the presence of H_2S [13], from the data presented here, it could be pointed out that the ternary alloy presented a higher hydrogen inhibition than the PdAu in CO_2 containing streams, probably related to the Ag surface segregation.

4. Conclusions

Both ternary alloy samples prepared using different deposition sequences, Pd-Ag-Au or Pd-Au-Ag, showed a complete alloy formation after exposure at 773 K and ΔP 10 kPa during 7 days. Despite the order of deposition, the samples exhibited similar hydrogen permeation flux at the same temperature and pressure.

In the presence of CO, the PdAgAu ternary alloy membranes showed a lower decrease of the hydrogen permeance compared with the binary PdAu alloy at 623 and 673 K. On the contrary, under CO_2 containing streams, the ternary alloy showed a higher decrease with a complete hydrogen recovery after removing CO_2 from the stream. When H_2S was introduced in the stream, a higher flux inhibition was observed on both PdAu and PdAgAu alloy membranes. After removal of H_2S, a hydrogen recovery of 60% and 76% was measured for the PdAu and PdAgAu membranes, respectively.

Upon exposure to CO containing streams both the $Pd_{82}Ag_{15}Au_3$–873 K-5 d and the $Pd_{78}Au_6Ag_{16}$–773 K-7 d samples showed a Pd enrichment at the surface. On the contrary, silver surface segregation after exposing the PdAgAu ternary alloy to a CO_2 containing stream was observed by XPS. This preferential segregation could induce the higher decrease on the hydrogen permeance in the ternary alloy.

Acknowledgments

The authors wish to acknowledge the financial support received from UNL (CAID 50320140300248LI), CONICET (PIP 292), and ANPCyT (PICT 1948). María Belén Gilliard is thanked for the XRF measurements.

References

[1] P. Nikolaidis, A. Poullikkas, A comparative overview of hydrogen production processes, Renew. Sustain. Energy Rev. 67 (2017) 597–611.
[2] N.A. Al-Mufachi, N.V. Rees, R. Steinberger-Wilkens, Hydrogen selective membranes: a review of palladium-based dense metal membranes, Renew. Sustain. Energy Rev. 47 (2015) 540–551.
[3] J.B. Hunter, Palladium alloy diffusion process for hydrogen purification, Platin. Met. Rev. 4 (1960) 130–131.
[4] J.B. Hunter, Silver-palladium film for separation and purification of hydrogen, U. S. Patent 2773561 A, 1956.
[5] L. Zhao, A. Goldbach, H. Xu, Tailoring palladium alloy membranes for hydrogen separation from sulfur contaminated gas streams, J. Membr. Sci. 507 (2016) 55–62.
[6] J.F. Gabitto, C. Tsouris, Sulfur poisoning of metal membranes for hydrogen separation, Int. Rev. Chem. Eng. 1 (2009) 394–411.
[7] T.A. Peters, T. Kaleta, M. Stange, R. Bredesen, Hydrogen transport through a selection of thin Pd-alloy membranes: membrane stability, H_2S inhibition, and flux recovery in hydrogen and simulated WGS mixtures, Catal. Today 193 (2012) 8–19.
[8] A.M. Tarditi, C. Imhoff, F. Braun, J.B. Miller, A.J. Gellman, L.M. Cornaglia, PdCuAu ternary alloy membranes: hydrogen permeation properties in presence of H_2S, J. Membr. Sci. 479 (2015) 246–255.
[9] A.E. Lewis, H. Zhao, H. Syed, C.A. Wolden, J.D. Way, PdAu and PdAuAg composite membranes for hydrogen separation from synthetic water-gas shift streams containing hydrogen sulfide, J. Membr. Sci. 465 (2014) 167–176.
[10] T.A. Peters, T. Kaleta, M. Stange, R. Bredesen, Development of ternary Pd-Ag-TM alloy membranes with improved sulphur tolerance, J. Membr. Sci. 429 (2013) 448–458.
[11] K.E. Coulter, J.D. Way, S.K. Gade, S. Chaudhari, G.O. Alptekin, S.J. DeVoss, S.N. Paglieri, B. Pledger, Sulfur tolerant PdAu and PdAuPt alloy hydrogen separation membranes, J. Membr. Sci. 405–406 (2012) 11–19.
[12] F. Braun, A.M. Tarditi, J.B. Miller, L.M. Cornaglia, Pd-based binary and ternary alloy membranes: morphological and perm-selective characterization in the presence of H_2S, J. Membr. Sci. 450 (2014) 299–307.
[13] F. Braun, J.B. Miller, A.J. Gellman, A.M. Tarditi, B. Fleutot, P. Kondratyuk, L.M. Cornaglia, PdAgAu alloy with high resistance to corrosion by H_2S, Int. J. Hydrog. Energy 37 (2012) 18547–18555.
[14] A.L. Mejdell, M. Jøndahl, T.A. Peters, R. Bredesen, H.J. Venvik, Effects of CO and CO_2 on hydrogen permeation through a ~ 3 μm Pd/Ag 23 wt% membrane employed in a microchannel membrane configuration, Sep. Purif. Technol. 68 (2009) 178–184.
[15] T.A. Peters, M. Stange, H. Klette, R. Bredesen, High pressure performance of thin Pd-23%Ag/stainless steel composite membranes in water gas shift gas mixtures; influence of dilution, mass transfer and surface effects on the hydrogen flux, J. Membr. Sci. 316 (2008) 119–127.
[16] A. Unemoto, A. Kaimai, K. Sato, T. Otake, K. Yashiro, J. Mizusaki, T. Kawada, T. Tsuneki, Y. Shirasaki, I. Yasuda, The effect of co-existing gases from the process of steam reforming reaction on hydrogen permeability of palladium alloy membrane at high temperatures, Int. J. Hydrog. Energy 32 (2007) 2881–2887.
[17] K. Hou, R. Hughes, The effect of external mass transfer, competitive adsorption and coking on hydrogen permeation through thin Pd/Ag membranes, J. Membr. Sci. 206 (2002) 119–130.
[18] M. Amano, C. Nishimura, M. Komaki, Effects of high concentration CO and CO_2 on hydrogen permeation through the palladium membrane, Mater. Trans. JIM 31 (1990) 404–408.
[19] F. Gallucci, F. Chiaravalloti, S. Tosti, E. Drioli, A. Basile, The effect of mixture gas on hydrogen permeation through a palladium membrane: experimental study and theoretical approach, Int. J. Hydrog. Energy 32 (2007) 1837–1845.
[20] M. Eriksson, L.-G. Ekedahl, Real time measurements of hydrogen desorption and absorption during CO exposures of Pd: hydrogen sticking and dissolution, Appl. Surf. Sci. 133 (1998) 89–97.
[21] S. Wieland, T. Melin, A. Lamm, Membrane reactors for hydrogen production, Chem. Eng. Sci. 57 (2002) 1571–1576.
[22] A. Li, W. Liang, R. Hughes, The effect of carbon monoxide and steam on the hydrogen permeability of a Pd/stainless steel membrane, J. Membr. Sci. 165 (2000) 135–141.
[23] F.C. Gielens, R.J.J. Knibbeler, P.F.J. Duysinx, H.D. Tong, M.A.G. Vorstman, J.T.F. Keurentjes, Influence of steam and carbon dioxide on the hydrogen flux through thin Pd/Ag and Pd membranes, J. Membr. Sci. 279 (2006) 176–185.
[24] H. Li, A. Goldbach, W. Li, H. Xu, CO_2 decomposition over Pd membrane surfaces, J. Phys. Chem. B 112 (2008) 12182–12184.
[25] A. Tarditi, C. Gerboni, L. Cornaglia, PdAu membranes supported on top of vacuum-assisted ZrO_2-modified porous stainless-steel substrates, J. Membr. Sci. 428 (2013) 1–10.
[26] A.M. Tarditi, F. Braun, L.M. Cornaglia, Novel PdAgCu ternary alloy: hydrogen permeation and surface properties, Appl. Surf. Sci. 257 (2011) 6626–6635.
[27] M. Engin Ayturk, E.A. Payzant, S.A. Speakman, Y.H. Ma, Isothermal nucleation and growth kinetics of Pd/Ag alloy phase via in situ time-resolved high-temperature X-ray diffraction (HTXRD) analysis, J. Membr. Sci. 316 (2008) 97–111.
[28] S. Hofmann, Depth profiling in AES and XPS, in: D. Briggs, M.P. Seah (Eds.), Practical Surface Analysis, Auger and X-ray Photoelectron Spectroscopy, Wiley, New York, 1990, pp. 143–255.
[29] A.M. Tarditi, C. Imhoff, J.B. Miller, L. Cornaglia, Surface composition of PdCuAu ternary alloys: a combined LEIS and XPS study, Surf. Interface Anal. 47 (2015) 745–754.
[30] D.A. Pacheco Tanaka, J. Okazaki, M.A. Llosa Tanco, T.M. Suzuki, Fabrication of supported palladium alloy membranes using electroless plating techniques, in: A. Doukelis, K. Panopoulos, A. Koumanakos, E. Kakaras (Eds.), Palladium Membrane Technology for Hydrogen Production, Carbon Capture and Other Applications. Principles, Energy Production and Other Applications, Woodhead Publishing, Sawston, Cambridge, 2015, pp. 83–99.
[31] N.S. Patki, S.-T. Lundin, J.D. Way, Rapid annealing of sequentially plated Pd-Au composite membranes using high pressure hydrogen, J. Membr. Sci. 513 (2016) 197–205.
[32] M.L. Bosko, E.A. Lombardo, L.M. Cornaglia, The effect of electroless plating time on the morphology, alloy formation and H_2 transport properties of Pd-Ag composite membranes, Int. J. Hydrog. Energy 36 (2011) 4068–4078.
[33] J.J. Conde, M. Maroño, J.M. Sánchez-Hervás, Pd-based membranes for hydrogen separation: review of alloying elements and their influence on membrane properties, Sep. Purif. Rev. 46 (2017) 152–177.
[34] H. Li, A. Caravella, H.Y. Xu, Recent progress in Pd-based composite membranes, J. Mater. Chem. A 4 (2016) 14069–14094.
[35] S. Abate, C. Genovese, S. Perathoner, G. Centi, Performances and stability of a Pd-based supported thin film membrane prepared by EPD with a novel seeding procedure. Part 1-behaviour in H_2:N_2 mixtures, Catal. Today 145 (2009) 63–71.
[36] A. Caravella, G. Barbieri, E. Drioli, Concentration polarization analysis in self-supported Pd-based membranes, Sep. Purif. Technol. 66 (2009) 613–624.
[37] I.-H. Svenum, J.A. Herron, M. Mavrikakis, H.J. Venvik, Adsorbate-induced segregation in a PdAg membrane model system: $Pd_3Ag(111)$, Catal. Today 193 (2012) 111–119.